Does Adsorption at Hydroxyapatite Surfaces Induce Peptide Folding? Insights from Large-Scale B3LYP Calculations

Albert Rimola,[†,‡] Massimiliano Aschi,[§] Roberto Orlando,[‡] and Piero Ugliengo*[‡]

[†]Departament de Química, Universitat Autònoma de Barcelona, 08193 Bellaterra, Spain

[‡]Dipartimento di Chimica, NIS Centre of Excellence and INSTM (Materials Science and Technology) National Consortium, University of Torino, Via P. Giuria 7, 10125 Torino, Italy

[§]Department of Chemistry, Chemical Engineering and Materials, University of L'Aquila, Via Vetoio (Coppito 1), 67010 L'Aquila, Italy

Ⓢ *Supporting Information*

ABSTRACT: Large-scale periodic quantum mechanical calculations (509 atoms, 7852 atomic orbitals) based on the hybrid B3LYP functional focused on the peptide folding induced by the adsorption on the (001) and (010) hydroxyapatite (HA) surfaces give interesting insights on the role of specific interactions between surface sites and the peptide, which stabilize the helix conformation over the "native" random coil ones for in silico designed model peptides. The two peptides were derived from the 12-Gly oligomer, with one (P1, C-tGGKGGGGGGEGGN-t) and two (P2, C-tGGKGGKEG-GEGGN-t) glutamic acid (E) and lysine (K) residue mutations. The most stable gas-phase "native" conformation for both peptides resulted in a random coil (RC) structure, with the helix (H) conformation being $\approx$100 kJ mol^{-1} higher in free energy. The two peptide conformations interact with the HA (001) and (010) surfaces by C=O groups via Ca^{2+} ions, by hydrogen bond between NH$_2$ groups and the basic PO$_4^{3-}$ groups and by a relevant fraction due to dispersion forces. Peptide adsorption was studied on the dry (001) surface, the wet one envisaging 2 H$_2$O per surface Ca^{2+} and, on the latter, also considering the adsorption of microsolvated peptides with 4 H$_2$O molecules located at sites responsible of the interaction with the surface. The P1 mutant does prefer to be adsorbed as a random coil by $\approx$160 kJ/mol, whereas the reverse is computed for P2, preferring the helix conformation by $\approx$50 kJ/mol. Adsorption as helix of both P1 and P2 mutants brings about proton transfer toward the HA surfaces with a large charge transfer component to the interaction energy.

INTRODUCTION

The biological activity of a given protein is partly due to its secondary structure and conformational state. Peptide chains are rather flexible so that the interest in finding novel ways that force the protein folding in a well-defined state has increased considerably. To be folded, a protein needs extra-interactions that compensate for the entropy loss associated with the folding of the polypeptide chain. Among the most common adopted constraint techniques, such as metal-ion complexation[1−5] or S—S bonds,[6−8] the interaction of proteins with inorganic surfaces has demonstrated to be a fruitful strategy to stabilize selected folded states.[9−19] This, nevertheless, remains a challenging goal since the protein−surface binding usually leads to denaturation and the loss of the biological functionality. Because of this, de novo peptide design techniques has emerged as a useful approach to assemble peptides with a defined structure and orientation on the surface,[20] as the synthetic peptide may contain, at very strategic positions, amino acidic residues that when in contact with the surface establish extra intermolecular interactions that drive and stabilize the folded protein.

The surface-induced peptide folding is a promising tool to (i) obtain peptide monolayers exhibiting free-interacting sequences that may display specific biochemical recognition phenomena and (ii) induce a specific bioactivity of the protein which is missing in its unfolded state. Both issues have several important applications in biosensing, biotechnology, biocatalysis, biomaterials, tissue engineering, nanotechnology, and proteomics. Interestingly, the peptide folding induced by mineral surfaces and the subsequent activation of a potentially "hidden" bioactivity might have triggered the first biocatalytic reactions in a primordial Earth (in absence of life), hence, giving rise to the emergence of the metabolic cycles, a crucial aspect for the origin of life.[21,22]

Several experimental studies performed with high-resolution spectroscopic techniques such as circular dichroism (CD) and solid state nuclear magnetic resonance (ssNMR) have been reported in the literature. They were focused on the formation of peptide secondary structures induced by the presence of surfaces and observed the formation of helical structures from synthetic peptides when interacting with hydrophobic surfaces[9] and cavities,[10] silica nanoparticles,[11,12] functionalized gold nanoparticles,[13,14] and hydroxyapatite (HA).[15] Such conformational changes have also been observed in natural proteins adsorbed on gold nanoparticles[16] and hydroxyapatite.[17−19] Despite the novelty of the works and the useful information provided, detailed atomistic features related to the binding mechanisms and the anchoring points between peptides and

the surfaces are very difficult to attain. One way to provide this missing information is by classical molecular dynamics-based studies,[23−26] focusing on the dynamic behavior of proteins in water and when docked to the surfaces. However, the adoption of classical force fields (FF), needed to handle the large number of atoms involved, inevitably lowers the accuracy of the results, as actual FF cannot cope with bond breaking/making which may indeed occur between side chain functionalities and the surfaces. One exception is by adopting a reactive force field like ReaxFF[27] which is able, by construction, to handle bond rupture/formation in a way mimicking quantum mechanical (QM) calculations. Indeed, very recently, Monti and co-workers[28] have extended ReaxFF to study the interaction of glycine and diglycine on the TiO_2 rutile (110) face using a newly ReaxFF force field for glycine.[29] QM calculations are the obvious choice to keep almost constant accuracy in the diverse situations occurring by these complex simulations, at the price of a very high computational cost.[25,26] For these reasons, we have adopted for this work CRYSTAL09 in its massive parallel version which is able to exploit hundreds of cores to solve the Schrödinger equation for periodic systems.[30]

We have been inspired by the work of Cappriotti et al.,[15] in which it was shown that a rich-γ-carboxyglutamic synthetic peptide assumes a random coil structure in solution, whereas it becomes reorganized into an α-helix when in contact with HA surfaces. Our target was to study such a process entirely in silico, by adopting a simplified version of the peptides and focusing on the two most common HA surfaces, namely, the (001) and the (010) ones. We chose the hybrid functional B3LYP[31] in a periodic context, adopting Gaussian basis sets of sufficiently high quality. Because of the complexity of the system and of high computational cost, we had to compromise on both the solvation state of the entire system and to limit the calculation to static optimization, as ab initio molecular dynamics (MD) would have been too computationally demanding. Our strategy was, first, to study the surface-induced folding process entirely in gas-phase and then to microsolvate the system with 8 water molecules at the sites responsible of the interactions for the gas-phase processes. In this way, the key role of the first solvation shell in crucial sites has been addressed. We are aware that this approach has serious limitations due to the above simplifications; notwithstanding, as it will be shown in the paper, a number of important energetic and structural details have been characterized.

■ METHODS

In the following, only essential computational details are provided, and a more extensive description is provided in the Supporting Information. All the periodic calculations for the interaction of the considered peptides with the HA (001) and (010) surfaces have been performed with the massive parallel version of the ab initio code CRYSTAL09,[32,33] which solves the Schrödinger equation for molecules, polymers, slabs and bulks using Gaussian basis sets. All the SCF calculations and geometry optimizations were performed with the B3LYP density functional method.[31,34] Geometry optimizations were performed using a Gaussian basis set of polarized double-ζ quality already adopted in previous studies.[35] Additionally, to increase the accuracy in computing the adsorption energies, single-point energy calculations on the optimized structures using the Ahlrichs and co-workers VTZP basis set[36] were carried out which, in addition, significantly reduces the BSSE as we demonstrated recently.[37] With the VTZP basis set, the number of atomic orbitals was 7852 which required distributing the Fock diagonalization over many cores.

Geometries were optimized by relaxing the internal coordinates within $P1$ symmetry keeping the lattice parameters fixed at the values of the optimized bare surfaces.

In a periodic treatment, the adsorption energy ΔE_{ads} per unit cell per adsorbate is defined as:

$$\Delta E_{ads} = E(SP//SP) - E(S//S) - E_m(P//P)$$

where $E(S//S)$ is the energy of a bare HA slab S in its optimized geometry, $E_m(P//P)$ is the molecular energy of a free peptide P in its optimized geometry, and $E(SP//SP)$ is the energy of the considered HA/P system in its optimized geometry (the symbol following the double slash identifies the optimized geometry at which the energy has been computed). ΔE_{ads} is a negative quantity for a bound system and can be recast in terms of deformation cost of the surface, the adsorbate, the lateral adsorbate−adsorbate interactions, and the interaction between the predeformed constituents. The final expression ΔE^C_{ads}, inclusive of the BSSE correction reads:

$$\Delta E^C_{ads} = \Delta E_{ads} + BSSE$$

It is worth mentioning that for periodic systems the BSSE can only be evaluated for cases in which both the adsorbate and the surface remains electro neutral, so that all processes in which bond making/breaking occurs are excluded. In this work, only adsorption of peptides in the random coil forms remain neutral when adsorbed (no proton transfer) and, accordingly, only for these cases, the BSSE have been computed. For the helix conformations, on the contrary, proton transfers do indeed occur preventing the BSSE evaluation. Notwithstanding, to keep balance between interaction energies, for the helix cases, the highest percentage of BSSE computed for the corresponding random coil cases was used to estimate the final ΔE^C_{ads} values.

B3LYP, as almost all standard hybrid and pure gradient corrected functionals, cannot cope with the dispersion energy component to the interaction energy, so that the empirical correction ΔD suggested by Grimme[38] and reparameterized by some of us for periodic systems,[39] has been added to the BSSE-corrected adsorption energies ΔE^C_{ads} in a posteriori fashion to obtain the final $\Delta E^C_{ads} + \Delta D$. In this way, the dispersive contribution is inserted in a non self-consistent way to the adsorption energy, which, somehow, underestimates its relevance (see also Supporting Information for more details).

Conformational study of peptide in the gas-phase at room temperature was performed using MD simulations with the Gromos 53a6 force-field[40] and the Gromacs package.[41] The peptide, initially folded and minimized in the helix conformation, was simulated for 160.0 ns with a time step of 2.0 fs at a temperature of 300.0 K kept constant with the Berendsen thermostat[42] with a time constant equal to the integration step. The LINCS algorithm[43] was used to constrain all the bonds. Conformational analysis was carried out using Essential Dynamics[44] by projecting the whole trajectory onto the subspace (essential space) constructed using the subset of eigenvectors, obtained by the all atoms covariance matrix diagonalization, characterized by the highest eigenvalues. This operation produces different basins of probability approximately corresponding to well-defined tridimensional peptide structures. Hence, the random-coil structure utilized in this work represented the most populated probability (lowest free energy) basin. Further details are provided in the Supporting Information.

■ RESULTS

In Silico Designed Peptides. The (001) and (010) HA surfaces are the most relevant ones from a biological viewpoint and have been chosen here as surface models to study the folding induced by the adsorption of the model peptides. HA has been chosen as a test system for two reasons: (i) it is the natural major inorganic constituent of bone and teeth and, accordingly, the natural choice to study biomolecule/biomaterial interactions; and (ii) the crystalline structure of HA $(Ca_{10}(PO_4)_6(OH)_2)$ exhibits calcium ions periodically

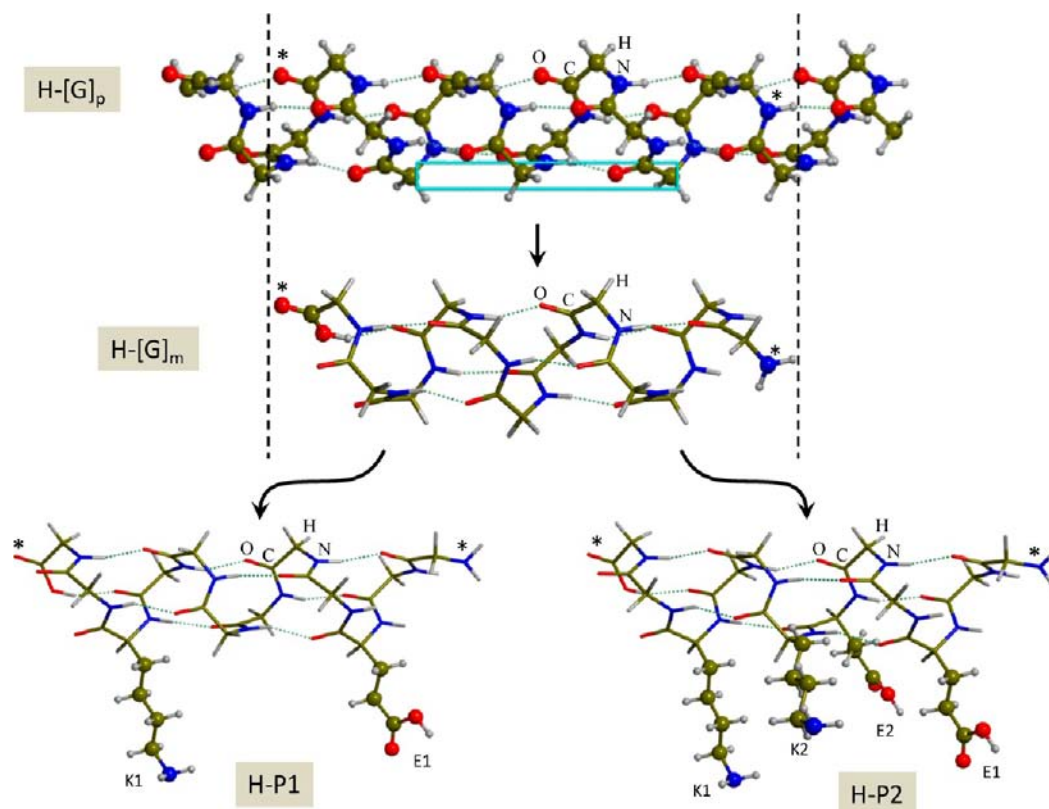**Figure 1.** Scheme for the in silico design of the helix structures. H-$[G]_p$, periodic helix polyglycine; H-$[G]_m$, a finite 12-mer glycine α-helix (terminus labeled by star character); H-P1, mutant with one glutamic acid and one lysine residues; H-P2, mutant with two glutamic acid and two lysine residues. For a proper interaction with the HA surfaces, the residues are oriented toward the same side of the main helix axis.

spaced at a distance close to the intervals of the repeating turns in an α-helix polypeptide. For point (ii), it is expected that sequences that contain residue side chains with a large Ca^{2+} affinity will interact favorably with the HA surfaces. Additionally, HA also contains phosphate groups, so that peptide residues containing groups behaving as H-bonding donors strongly interact with the HA surfaces. In summary, amino acids containing either acidic or basic residues are expected to have high affinity for the HA surfaces.

Indeed, calculations in both gas-phase and under microsolvation conditions (few water molecules) carried out by some of us show that single amino acids either acidic (namely, aspartic and glutamic acids) or basic (namely, lysine and arginine) interact strongly with HA surfaces.[35,45−48] This is in agreement with experimental measurements indicating that electrostatic complementary between protein and the surface fields is the leading force that drives the adsorbate to the surface, eventually causing the protein to fold as a helix.[11−15]

To study a possible role of the HA surfaces on the protein folding, we designed an in silico Gly polymer in its α-helix conformation, as shown in Figure 1. We first optimized the geometry of the surface-free polyglycine whose unit cell contains 7 independent Gly residues (linear group, $P1$). The resulting optimized structure (Figure 1, H-$[G]_p$ structure), is indeed a perfect α-helix with the typical $i + 4 \rightarrow i$ H-bonds feature. The infinite helix was then cut to define a small peptide with 12-Gly residues (structure H-$[G]_m$, Figure 1), showing three helical turns. The dangling bonds resulting from the polymer to the 12-mer transformation have been healed by H (NH_2 terminus) and OH (COOH terminus), labeled by asterisks in Figure 1. The choice of 12-mer is consistent with

the size of the HA cell chosen to represent the (001) and (010) surfaces (12-mer length of 22 vs 24 Å for the diagonal of the HA surface cell). The 12-Gly polypeptide is highly hydrophobic, so in order to provide residues apt to interact with the HA surfaces (vide supra), the peptide has been mutated by substituting some of the Gly with glutamic acid (E) and lysine (K). In one mutant (P1, C-tGGKGGGGGGEGGN-t), Figure 1) only one E and K residues were added, while in the other (P2, C-tGGKGGKEGGEGGN-t), Figure 1) two E and K were included. To maximize the interactions with the HA surfaces, the E and K residues occupy positions in which their side chains remains on the same side of the main helix axis (see Figure 1).

Surface-Free Gas-Phase Helix Folding. The optimized helix forms of P1 and P2 in gas phase are shown in Figure 2a (H-P1) and Figure 2b (H-P2), respectively. They resulted from the optimization of the mutated peptides as cut out from the periodic polyglycine. The structure of H-P1 has five consecutive $i + 3 \rightarrow i$ H-bonds and three consecutive $i + 4 \rightarrow i$ ones; structure H-P2 shows three consecutive $i + 3 \rightarrow i$ H-bonds and five consecutive $i + 4 \rightarrow i$ H-bonds. Thus, peptides exhibit a mixture of 3_{10} and α-helix structures, as shown by the triangular and square shapes associated to the 3_{10} and α-helix structures, respectively (Figure 2c−f). Any attempt to convert the E and K residues in a zwitterionic state (by imposing KH^+ and E^- states) resulted in a spontaneous proton transfer back to restore the neutral K and E residues. This is in agreement with what is known about gas-phase instability of the zwitterionic form of free amino acids.[49]

The method so far adopted forced the peptide to assume a helix conformation by construction. However, one has to
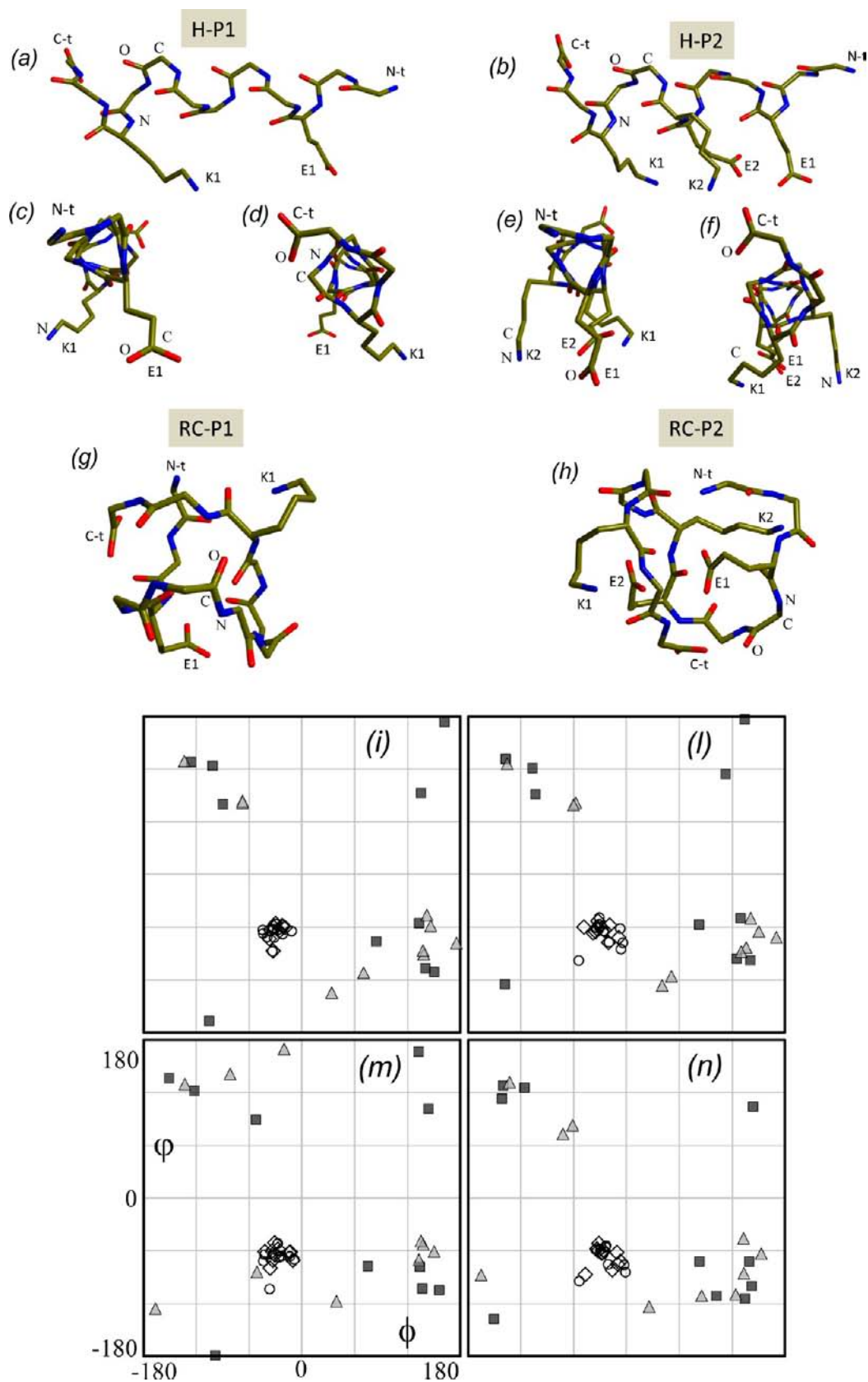
Figure 2. Top: (a and b) H-P1 and H-P2 optimized helix structures viewed normal to main helix axis. (c/d and e/f) Same as panels a and b viewed along the main helix axis. Region nearby the N-t and C-t adopt 3_{10} and α-helix structures, respectively. (g and h) Skeleton view of the P1 and P2 optimized structures in their "native" random coil conformations. Bottom: Ramachandran plots of gas-phase P1 and P2 peptides in their helix H-P1 (empty diamond), H-P2 (empty circle), and random coil RC-P1 (filled square), RC-P2 (filled triangle) conformations as: (i) free gas-phase; (l) adsorbed on HA (001) surface; (m) adsorbed on HA (010) surface; (n) adsorbed on wet HA(001)/W8 surface (two H_2O per Ca^{2+}) .

establish whether this conformation is the most stable one for the free P1 and P2 peptides. An exhaustive conformational search by means of classical MD simulations of both peptides have been run in gas-phase conditions to determine the most stable conformation. Results showed that both peptides prefer a random coil conformation (RC-P1 and RC-P2, Figure 2g and h, respectively) over the starting helix one. A Ramachandran plot of the ϕ and Ψ torsion angles for the four peptides (H-P1, H-P2, RC-P1, RC-P2) (Figure 2i) confirms that H-P1 and H-P2 values are within the region of the helix, whereas RC-P1 and RC-P2 values are filling the whole region, showing character of random coil.

The random coil peptides obtained from the MD calculations have then been fully optimized at B3LYP level, so that the reaction energy ΔE_{rx} of RC-P1 → H-P1 and RC-P2 → H-P2 processes have been computed (see Table 1). QM

Table 1. Reaction Energies (Electronic ΔE_{rx}, Enthalpies ΔH_{rx}, and Gibbs ΔG_{rx}) for the Conversion of Peptides from Their Random Coil Structures to Helix Forms in Gas Phase[a]

folding process	ΔE_{rx}	ΔD	$\Delta E_{rx} + \Delta D$	$\Delta H_{rx} + \Delta D^b$	$\Delta G_{rx} + \Delta D^b$
RC-P1 → H-P1	45.1	48.9	94.0	78.3	101.7
	(49.6)	(48.9)	(98.5)	(82.8)	(106.2)
RC-P2 → H-P2	52.1	31.0	83.1	72.4	93.6
	(56.0)	(31.0)	(87.0)	(76.3)	(97.5)

[a]Data computed at B3LYP/VTZP on structures optimized at B3LYP/double-ζ polarized level. Values in parentheses are for fully B3LYP/VTZP optimized structures. Units in kJ mol^{-1}. [b]Values computed by adding to the $\Delta E_{rx} + \Delta D$ values the enthalpic and entropic corrections obtained from frequency calculations performed at B3LYP/double-ζ level and $T = 298$ K.

data showed that the folding of both peptides from random coil to helix is endoenergetic ($\Delta E_{rx} > 0$). The addition of the dispersion contribution to the pure B3LYP energies (ΔD column, Table 1) further increases the endoenergetic character of the processes ($\Delta E_{rx} + \Delta D$ column, Table 1). The entropic contribution computed by standard statistical mechanics formulas using the harmonic vibrational frequencies should be considered as roughly approximated as it does not include neither the anharmonicity character of many modes characterized by large amplitude motion nor the configuration entropy due to conformations close in energy. Explorative calculations run with classical MD (see Supporting Information Figure S1) revealed, however, that these factors are less important in gas phase than in water. Within these approximations, the ($T\Delta S$) resulted in a negative value (about -20 kJ mol^{-1}), in agreement with the lower entropy content of the helix compared to the random coil. The final free reaction energies inclusive of the dispersive contribution are around 100 kJ mol^{-1}, irrespective of the mutants. Data in Table 1 also show the very good agreement between the reaction energy computed with cheap single point energy calculations at B3LYP/VTZP//B3LYP/double-ζ polarized basis set and those computed with the expensive fully optimized B3LYP/VTZP ones. Because of that, the subsequent energy evaluations have all been carried out as single point B3LYP/VTZP//B3LYP/double-ζ polarized basis set calculations.

Structures and Energetics of Peptides Adsorbed on Dry HA Surfaces. Previous results established, on a firm base, that the random coil conformation is more stable than the helix one for the considered gas-phase peptides. We have then

studied whether the adsorption on the HA (001) and (010) surfaces may change the energetics of the considered reactions. Our previous experience[35,45,46,48] indicates that the peptide/HA interactions are dictated partly by specific electrostatic interactions. For the helix forms, specific interactions of the K and E side chains with the Ca^{2+} and PO$_4^{3-}$ surface groups are obviously the dominant ones. For the random coil peptides, due to the more compact structure, the most favorable sites of interactions with the surfaces are not self-evident. For these cases, we have computed the electrostatic potential maps (EPMs) of all the random coil peptides (Supporting Information Figure S2) and used the electrostatic complementarity between the electric features of the peptide and that of the clean HA surfaces to properly dock the peptides toward the surface. The present approach does not consider at all the obvious fact that the most stable conformation adopted by the peptide in gas phase may be different from the one adopted on the HA surfaces. In essence, an exhaustive conformational search for the peptide on the HA would have been required in a more rigorous approach. Clearly, this would have been extremely demanding even for classical force field calculations and impossible to perform with our approach based on static minimization calculations.

The resulting structures for the RC-P1 and RC-P2 forms interacting with the HA (001) and (010) surfaces are shown in Figures 3 and 4, respectively. The interactions between the peptides and the HA surfaces are through two C=O groups belonging to the backbone chain of the peptides and Ca^{2+} ions of the surfaces. These carbonyl groups are those exhibiting the deepest negative electrostatic potentials in the EPMs (Supporting Information Figure S2). H-bond interactions between protons belonging to the NH backbone groups or
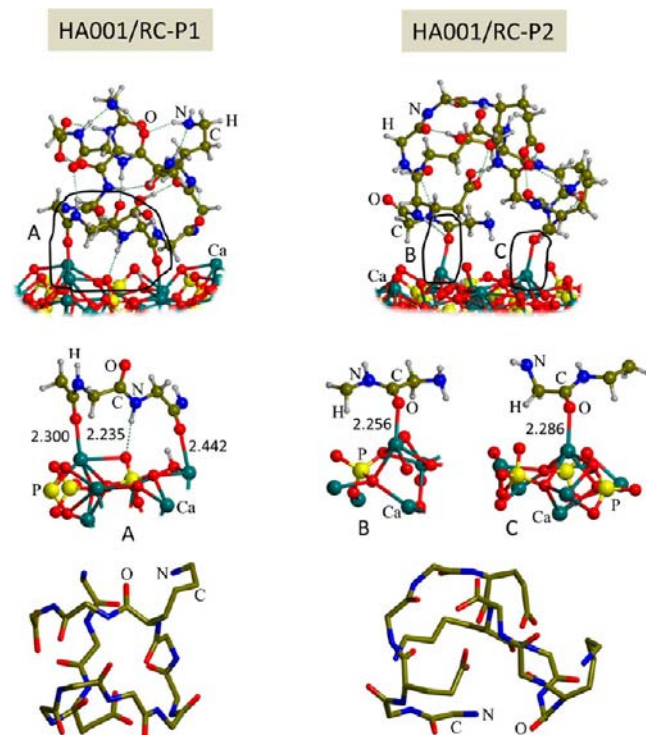

Figure 3. B3LYP optimized structures of RC-P1 and RC-P2 adsorbed on the (001) hydroxyapatite surface. Insets A−C highlight the shortest intermolecular contacts between peptides and the surface atoms. Bottom: backbone only view of the adsorbed peptides.
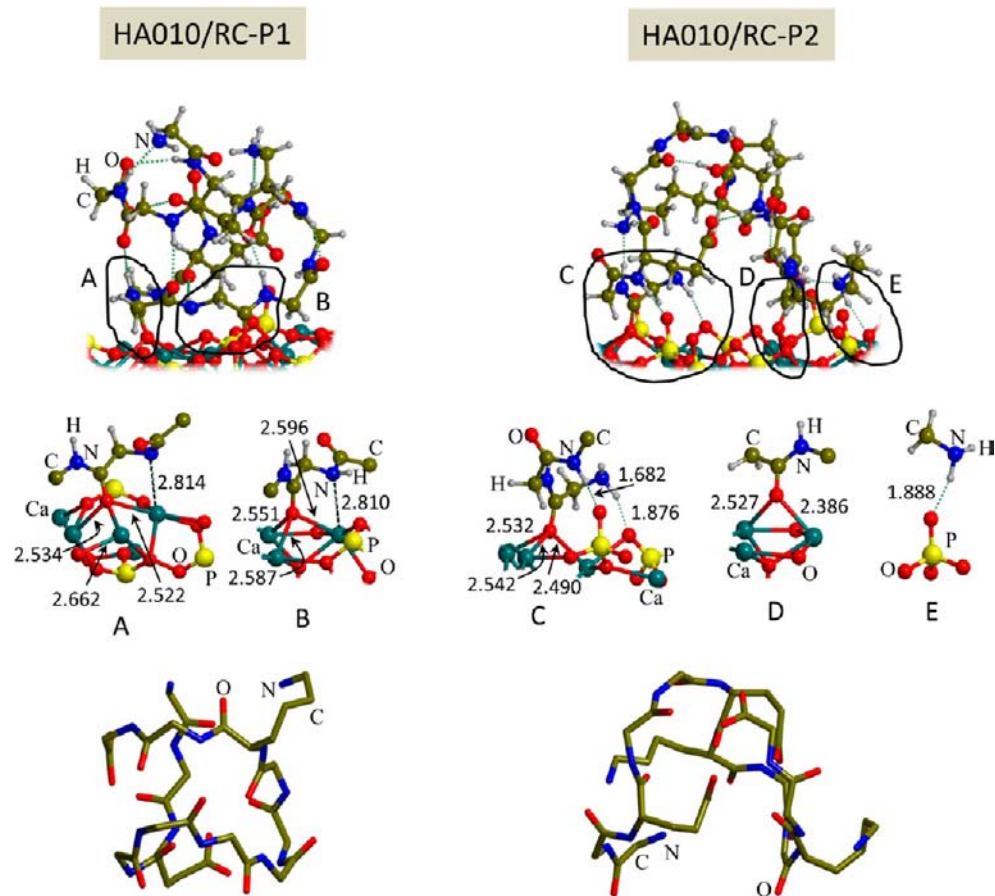
Figure 4. B3LYP optimized structures of RC-P1 and RC-P2 adsorbed on the (010) hydroxyapatite surface. Insets A−E highlight the shortest intermolecular contacts between peptides and the surface atoms. Bottom: backbone only view of the adsorbed peptides.
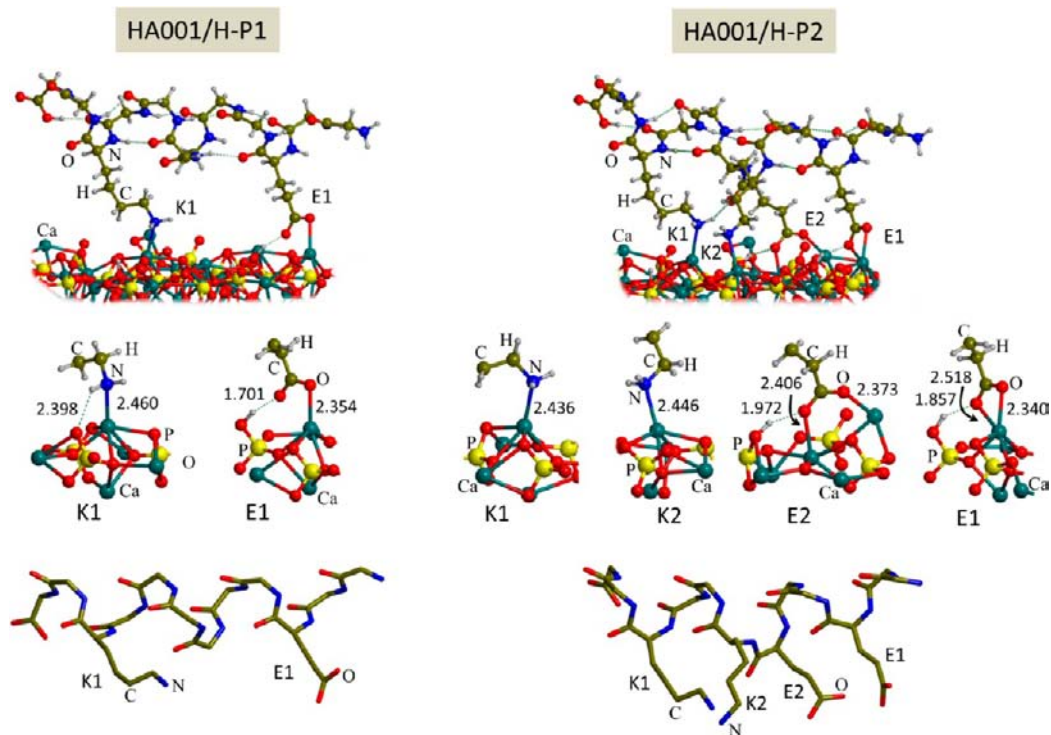

Figure 5. B3LYP-optimized structures of H-P1 and H-P2 adsorbed on the (001) hydroxyapatite surface. Insets K1, K2, E1, and E2 highlight the shortest intermolecular contacts between peptides and the surface atoms. Bottom: backbone only view of the adsorbed helix peptides.

Figure 6. B3LYP optimized structures of H-P1 and H-P2 adsorbed on the (010) hydroxyapatite surface. Insets K1, K2, E1, and E2 highlight the shortest intermolecular contacts between peptides and the surface atoms. Bottom: backbone only view of the adsorbed helix peptides.
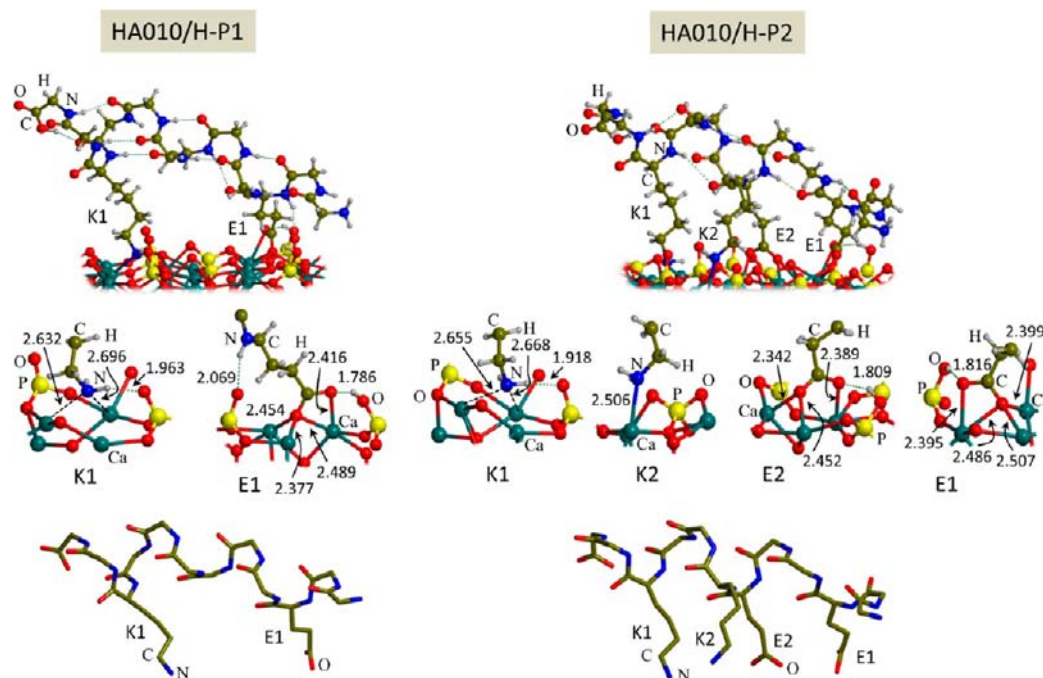
to the NH_2 groups and the phosphate surface O atoms are also established. Geometrical details are shown in Figure 3 and 4.

Figures 5 and 6 show the structures of the H-P1 and H-P2 peptides when adsorbed on the HA (001) and (010) surfaces. As anticipated (vide supra), the peptide groups interacting with the surfaces belong to the K and E amino acidic residues, that is, NH_2 and COOH, respectively. Significantly, for the COOH groups belonging to the E residues, spontaneous proton transfer toward the surface PO_4 groups occurs, leading to the formation of strong H-bond interactions between the protonated phosphate and the resulting COO^- groups. Proton transfer processes have already been predicted for glycine and glutamic acid interacting with HA surfaces.[35,45,47,48] It is worth noting that the proton transfer process would have not been predicted by using classical force field as bond making/breaking is not taken into account. The proton transfer has important effects on the interaction energy as, for the helix cases, an extra charge−charge component to the interaction between the negative peptide and the positive HA surface takes place. Indeed, by using Mulliken charges, it turned out that the H-P1 exhibits a net charge of $-0.8450\ e$ due to the proton transfer toward the HA(001) surface (which becomes positively charged by the same amount to ensure electro neutrality). For the adsorption of the H-P2 case, the net charge ($-1.800\ e$) is almost doubled with respect to the H-P1 peptide due to the presence of two E groups releasing their protons to the surface. For the HA(010) surface, the above net charge values are higher (in absolute term), namely, -1.3666 and -2.5103 electrons. The reason for the charge transfer enhancement when passing from HA(001) to HA(010) is revealed by inspection of the geometries of Figures 5 and 6, respectively. For the HA(001), the NH_2 group of the K residue only interacts through the N lone pair, releasing electronic charge toward the surface (inset K1 and K2, Figure 5). For the HA(010), on the contrary, a strong H-bonding is established between the NH bond and the surface basic oxygen which

reverse the flux of charge (inset K1, Figure 6) and account for the higher charge transfer. Interestingly, for the random coil RC-P1/RC-P2 cases, the net charges are far smaller (in absolute term): $-0.1141/-0.0047\ e$ and $-0.4281/-0.5918\ e$ for the HA(001) and HA(010) surfaces, respectively. Irrespective on the folding conformation, the number of interactions involving Ca^{2+} ions is higher for HA (010) surface compared with the (001) one, as the former is known to be more reactive.[35,50] One delicate point is whether the helix structure is disrupted by the strong interactions with the HA surfaces. As Figures 5 and 6 show, the helix conformation is highly conserved upon interaction with the HA surfaces, which is also highlighted by the Ramachandran plot (Figures 2l and 2m, respectively).

The energetic features of the peptides adsorption have been collected in Table 2. The $\Delta E^C_{ads} + \Delta D$ values are all large and negative, that is, the peptide adsorption on both HA surfaces are highly exoenergetic. The most favorable ones are obtained on the HA (010) surface, with values almost doubled with respect to the HA (001) surface, in agreement with the higher reactivity of the former compared to the latter.[35,45] An important trend in the computed adsorption energy is shown by data of Table 2: both RC-P1 and RC-P2 exhibit close $\Delta E^C_{ads} + \Delta D$ values, that is, they do not depend much on the kind of mutant. The similarity is striking for the HA (001) case and less so for the HA (010) one. In contrast, H-P1 and H-P2 show large differences in the adsorption energy, with the most negative values for the H-P2 case, irrespective of the considered HA surface. The reasons are simple: for the random coil cases, the interactions occurring between the Ca^{2+} ions and C=O carbonyl groups of the peptides backbone are all very similar. For the helix cases, on the contrary, because the interactions are through the E and K residues, it is obviously more favorable for H-P2 exhibiting four residues compared to only two for H-P1 (see Figures 5 and 6). Dispersive contribution to the interactions (ΔD, Table 2) is also remarkable, particularly for

Table 2. Adsorption of Dry P1 and P2 Peptides on Dry HA(001) and HA(010) Hydroxyapatite Surfaces (H)[a]

adsorption process	ΔE_{ads}	ΔE^C_{ads}	% BSSE	ΔD	$\Delta E^C_{ads} + \Delta D$
		HA(001) Dry Surface			
H + RC-P1 → H/RC-P1	−179.1	−93.6	48	−144.1	−237.7
H + RC-P2 → H/RC-P2	−232.9	−144.2	38	−101.5	−245.7
H + RC-P1 → H/H-P1	−306.3	−159.3[b]	48	−19.9	−179.2
H + RC-P2 → H/H-P2	−530.5	−275.9[b]	48	−85.8	−361.7
		HA(010) Dry Surface			
H + RC-P1 → H/RC-P1	−499.1	−281.8	43	−210.5	−492.3
H + RC-P2 → H/RC-P2	−523.9	−308.8	41	−237.7	−546.5
H + RC-P1 → H/H-P1	−546.4	−311.4[b]	43	−145.7	−457.1
H + RC-P2 → H/H-P2	−911.2	−519.4[b]	43	−240.5	−759.9

[a]ΔE_{ads} and ΔE^C_{ads} as non-corrected and BSSE corrected interaction energies, respectively. RC-P1, RC-P2, and H-P1 and H-P2 label the random coil and helix peptide conformations, respectively. %BSSE is the adopted BSSE percentage to the ΔE_{ads}, ΔD is the dispersion contribution, and $\Delta E^C_{ads} + \Delta D$ is the final adsorption energies inclusive of dispersion. Units in kJ mol^{-1}. [b]Estimated ΔE^C_{ads} values obtained by assuming the highest BSSE percentage computed for the RC systems. The actual ΔE^C_{ads} values cannot be computed due to the deprotonation of the helix upon HA adsorption (see Methods section for more details).

the RC peptides in comparison with the H ones. For the former, the ΔD values are more negative due to the closeness of the random coil peptides to the HA surfaces compared to the helix structures, with the exception of H-P2 on the HA (010) surface (see Figures 5 and 6). Despite the adoption of a rather flexible polarized triple-ζ basis set, the BSSE is still rather large and has been accounted for to improve the accuracy of the adsorption energy.

As it has been shown in the previous section, the zwitterionic form of the free P1 and P2 peptides is unstable with respect to the neutral form. An interesting point is to establish whether the adsorption may stabilize the zwitterionic form. Results are shown in Supporting Information Table S1, limited to the adsorption of the helix conformers only. The interaction energies are almost identical for the H-P1 and in favor of the neutral form for the H-P2 case. The corresponding structures are shown in the Supporting Information Figure S3. The mechanism of interaction is different with respect to the neutral case, as the NH_3^+ establishes three H-bonds with the basic oxygen of the surface while the COO^- bridges two Ca^{2+} surface ions.

Structures and Energetics of Peptides Adsorbed on Microsolvated HA Surfaces. As anticipated, the present study cannot be extended by including a large number of water molecules to mimic the role of solvation on the considered processes, due to the exceedingly high computational cost. A simple algorithm based on distance criteria has been used to compute the number of H_2O molecules that would be needed to dress the adsorbed peptides up to a second solvation shell, resulting in about 100 H_2O molecules which is outside the capability of the present approach. A further complication to handle a high number of water molecules is the change in the

canonical state of the amino acids with a probable stabilization of zwitterions originating by proton transfer from Glu toward Lys amino acids. Nonetheless, to at least account for the relevance of water interaction on the most actives sites, the adsorption of P1 and P2 has been studied in a microsolvation regime, that is, in presence of 8 H_2O molecules preadsorbed at the HA (001) surface only. Indeed, for the HA (010) surface, water spontaneously dissociates,[51] which would render the calculations rather complex due to important reconstruction of the pristine (010) surface upon H_2O adsorption. The 8 H_2O molecules were adsorbed in pairs on the most exposed Ca^{2+} ions of the HA(001) surface (Supporting Information Figure S4), reducing the Lewis acidity of these sites compared to the pristine surface. The optimized structures are shown in Figures 7 and 8. For the random coil peptides (Figure 7), the interactions are similar to those occurring in dry conditions (vide supra), with the $Ca^{2+} \cdots O = C$ interactions still existing despite the water molecules directly interacting with the same Ca^{2+} ion: the only change was a longer Ca−O bond distances compared to the adsorption on dry conditions. For the HW/RC-P1 case (HW=HA(001)/8W, wet surface), the presence of water induced the formation of a new $Ca^{2+} \cdots NH$ bond by establishing a H-bond with a nearby NH peptide group bringing the N atom close enough (2.650 Å) to a nearby surface Ca^{2+} ion (see region A, Figure 7).

The helix/HA surface structures are also very similar to those resulting by adsorption on dry surfaces as the binding through the K and E residues still involved Ca−N and Ca−O electrostatic interactions. Noticeably, proton transfers from the COOH groups still occurred followed by H-bonding between the surface proton and the O atom of the carboxylate moiety. As for the adsorption on dry surfaces, the P1 and P2 mutants still maintain their helix conformation as shown by Figure 8 and by the Ramachandran plot (Figure 2n).

Table 3 reports the energetic features for the adsorption process of P1 and P2 to the wet HA (001) surface. The adsorption energies are all negative showing again the exoenergetic character of the adsorption processes. Charge transfer is also very similar to that computed for the dry HA(001) surface for both random coil and helix conformations (see Supporting Information Table S2). Comparison with data of Table 2 for the adsorption on dry surfaces reveals a rather subtle effect played by the adsorbed H_2O on differentiating between random coil and helix peptides. Indeed, the interaction energies are more negative for the random coil structures for the wet surfaces compared to the dry ones, whereas the reverse resulted for the helix case. This was caused by the energetic balance between the cost of displacing water from the Ca^{2+} ions and the gain due to the new H-bond interactions established by H_2O with the adsorbed peptide.

The next step toward a more realistic situation was to add four H_2O molecules to microsolvate the interaction sites of the random coil and helix peptides (optimized structures in Supporting Information Figure S5). To simplify the calculations, we computed the new interaction energies considering as reactants, the solvated peptide *plus* the solvated HA (001) surface and, as products, the former peptide adsorbed on the solvated HA (001) surface *plus* four free H_2O molecules derived from desolvating the peptide and being incorporated in the surrounding water. In this way, data on the lowest half of Table 3 include the cost of desolvating the peptide induced by the surface interaction. The interaction energies are still all negative (exoenergetic reactions) but the absolute values are all
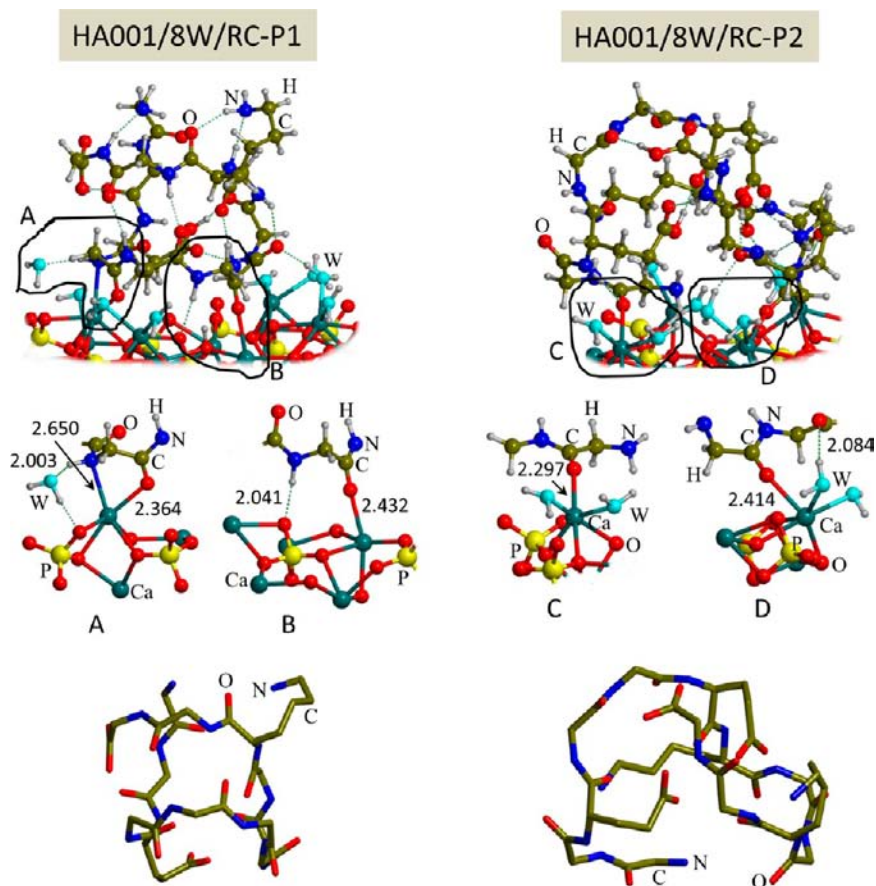
Figure 7. B3LYP-optimized structures of RC-P1 and RC-P2 adsorbed on the wet (001) hydroxyapatite surface (8 H_2O molecules). Water molecules labeled by W and color coded in cyan. Insets A−D highlight the shortest intermolecular contacts between peptides and the surface atoms. Bottom: backbone only view of the random coil adsorbed peptides.
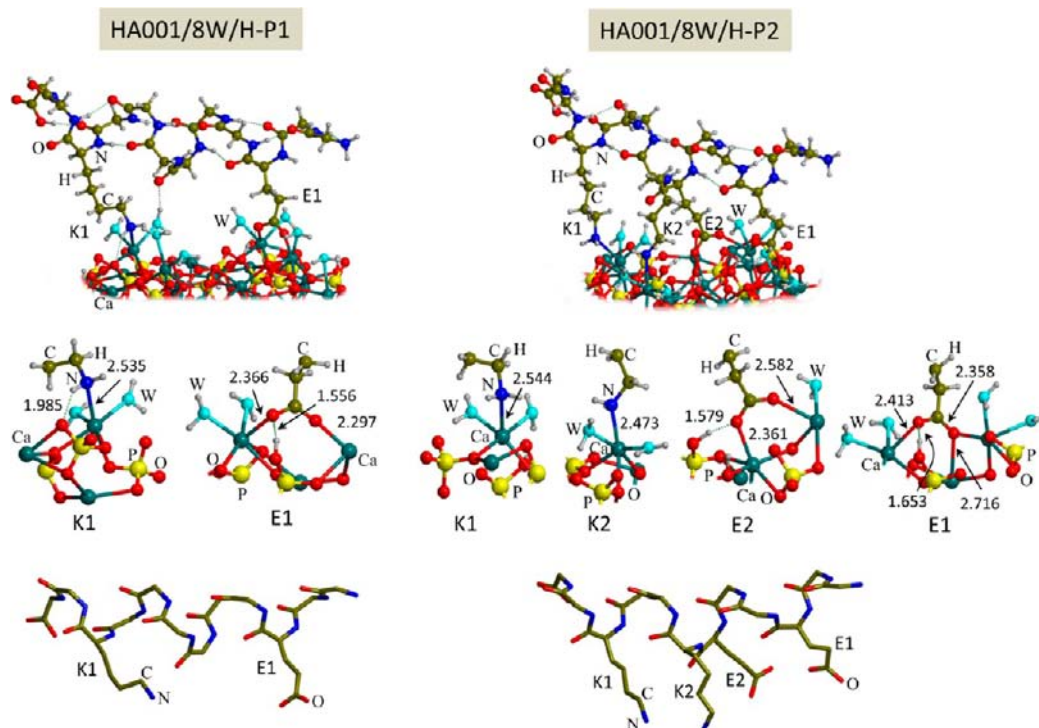

Figure 8. B3LYP optimized structures of H-P1 and H-P2 adsorbed on the (001) hydroxyapatite surface (8 H_2O molecules). Water molecules labeled by W and color coded in cyan. Bottom: backbone only view of the adsorbed helix peptides.

Table 3. Adsorption of Dry and Wet (4 H$_2$O per Peptide) P1 and P2 Peptides on Microsolvated (8 H$_2$O per Unit Cell) HA(001) Hydroxyapatite Surfaces (HW)^a

adsorption process	ΔE_{ads}	adsΔE^C	% BSSE	ΔD	$\Delta E^C_{ads} + \Delta D$
Wet HA(001) Surface/Dry Peptide					
HW + RC-P1 → HW/RC-P1	−202.4	−128.4	37	−171.4	−299.8
HW + RC-P2 → HW/RC-P2	−195.9	−139.3	29	−169.1	−308.4
HW + RC-P1 → HW/H-P1	−200.5	−126.3^{b,c}	37	−20.4	−146.7
HW + RC-P2 → HW/H-P2	−371.5	−234.0^{b,c}	37	−121.4	−355.4
Wet HA(001) Surface/Wet Peptide					
HW + RC-P1/4W → HW/RC-P1 + 4W	−31.4	−19.8^{b,c}	37	−134.9	−154.7
HW + RC-P2/4W → HW/RC-P2 + 4W	−15.4	−9.7^{b,c}	37	−122.3	−132.0
HW + RC-P1/4W → HW/H-P1 + 4W	−29.5	−18.6^{b,c}	37	+16.1	−2.5
HW + RC-P2/4W → HW/H-P2 + 4W	−191.0	−120.3^{b,c}	37	−74.6	−194.9

^{a}ΔE_{ads} and ΔE^C_{ads} as non-corrected and BSSE corrected interaction energies, respectively. RC-P1, RC-P2, H-P1, and H-P2 label the random coil and helix peptide conformations, respectively. %BSSE is the adopted BSSE percentage to the ΔE_{ads}, ΔD is the dispersion contribution, and $\Delta E^C_{ads} + \Delta D$ is the final adsorption energies inclusive of dispersion. Units in kJ mol^{-1}. ^{b}Estimated ΔE^C_{ads} values obtained by assuming the highest percentage of BSSE computed for the RC systems. ^{c}The actual ΔE^C_{ads} values cannot be computed due to the deprotonation of the helix upon HA adsorption (see Methods section for more details). ^{c}The actual ΔE^C_{ads} values cannot be computed due to the expulsion of 4 water molecules.

much smaller than the data not envisaging peptide solvation (data on the highest half of Table 3) and those for the adsorption on dry surfaces (see Table 2). It is worth noting that the main order of stability between the considered processes is the same for the most realistic process (data of Table 3) compared with reactions carried out in dry conditions (data of Table 2), supporting the validity of the latter approach.

Data from Tables 2 and 3 can be combined in such a way to highlight the relative affinity toward the HA(001) surface of the random coil versus the helix conformation. Table 4 shows that the adsorption of the random coil RC-P1 on both dry and wet HA (001) and HA (010) surfaces is preferred over the H-P1 by a significant amount. The situation changes when the P2 is involved: in all cases, the H-P2 is preferred over the random coil case. These trends are the same also when free energies are computed by correcting the electronic energies with the standard statistical mechanics formulas based on the adoption of harmonic frequencies computed for the free peptides in the two forms. The main message is that P2 can be stabilized as a helix by the HA surface over its most stable random coil form, at variance with the case of P1. The reasons are due to a higher number of "active sites" present in P2 with respect to P1, which can interact more strongly via a subtle interplay between dispersive, electrostatic and H-bond interactions on the HA surface sites. This conclusion remains effective also when water solvation is accounted for by means of a limited number of explicit water molecules.

Table 4. Folding Energies (Electronic ΔE_{rx}, Enthalpies ΔH_{rx}, and Gibbs ΔG_{rx}) for the P1 and P2 Peptides Induced by the Adsorption at the Dry HA (001) and (010) Surfaces (H) and on the Wet HA (001) One (HW═HA(001)/8W)^a

folding process	$\Delta E_{rx}{}^b$	$\Delta H_{rx}{}^c$	$\Delta G_{rx}{}^d$
HA(001) Dry Surface			
H/RC-P1 → H/H-P1	+58.5	+42.8	+66.1
H/RC-P2 → H/H-P2	−116.0	−126.7	−105.5
HA(010) Dry Surface			
H/RC-P1 → H/H-P1	+35.2	+19.5	+42.8
H/RC-P2 → H/H-P2	−213.4	−224.1	−202.9
HA(001)/W8 Wet Surface			
HW/RC-P1 → HW/H-P1	+152.2	+136.5	+159.8
HW/RC-P2 → HW/H-P2	−62.9	−73.6	−52.4

^{a}RC-P1, RC-P2, H-P1, and H-P2 label the random coil and helix peptide conformations, respectively. Units in kJ mol^{-1}. ^{b}From the corresponding $\Delta E^C_{ads} + \Delta D$ values. ^{c}From the corresponding $\Delta E^C_{ads} + \Delta D$ values, including the enthalpic corrections obtained from the free-surface processes (Table 1). ^{d}From the corresponding $\Delta E^C_{ads} + \Delta D$ values, including the entropic corrections obtained from the free-surface processes (Table 1).

■ CONCLUDING REMARKS

The capability of HA (001) and (010) surfaces to adsorb a peptide model and drive its conformation from the most stable random coil in gas phase to a helix due to adsorption has been studied by means of quantum mechanical B3LYP calculations carried out on periodic models of the HA surfaces. Two short peptides (P1 and P2) made by 12 amino acidic residues (P1, C-tGGKGGGGGGGEGGN-t; P2, C-tGGKGGKEGGEGGN-t) have been designed in silico for this purpose and their preferred conformation in gas phase has been established first, by classical molecular dynamics simulation, and then by full quantum mechanical B3LYP optimization. Exhaustive search revealed that the preferred conformation for both peptides was a random coil one, the helix ones being ≈100 kJ mol^{-1} higher in energy. The main reasons for the random coil stability are the higher number of intramolecular H-bonds and more effective dispersive interactions due to its compactness compared to the helix. Adsorption of P1 and P2 peptides on the HA (001) and (010) surfaces is exoenergetic for both random coil and helix conformations and for both surfaces, the (010) one showing more negative interaction energies than the (001) one. Addition of 8 H$_2$O molecules on the most active Ca^{2+} sites (two H$_2$O per surface Ca^{2+}) at the HA (001) surface does not hinder the adsorption process, which remains exoenergetic for all cases. Despite the reduced Lewis acidity of the hydrated Ca^{2+} ions, the peptides are still able to interact with the Ca^{2+} ions by displacing the H$_2$O molecules, these latter engaging new H-bonds with the adsorbed proteins. For the peptides adsorbed as random coil, the interactions are between C═O backbone groups and surface Ca^{2+} ions with large and favorable dispersive interactions of similar strength. The situation is entirely different when the peptides are adsorbed as helix, since the important interactions are through the K and E amino acidic residues (i.e., establishing two and four contact points for P1 and P2, respectively) and dispersion forces, which are more relevant for H-P2 than for H-P1. The charge transfer is very large for the adsorption of P1 and P2 as helix on both surfaces is either dry or wet and less so when adsorbed as random coil. The charge transfer is dominated by the occurrence of the proton transfer and by the strength of the

H-bonds between peptides and the HA surfaces which would have been missed by the adoption of classical force fields. To come close to more realistic conditions, also the peptides have been microsolvated using four H_2O molecules which implied a further desolvation cost after adsorption at the HA surfaces. All in all, the balance between the energetic cost of passing from random coil to helix, to displace the preadsorbed H_2O at the HA surface together with the protein desolvation and the energy gain due to the protein/surface interactions is in favor of adsorption in all cases, with the HW + RC-P1/4W → HW/H-P1 + 4W process being at the limit of exoenergeticity. When equilibrium between adsorbed random coil and helix peptides is established, P1 prefers to stay adsorbed as a random coil, at variance with P2 for which the adsorption on HA (001) surface favors the helix conformation.

In conclusion, for the helix stabilization to occur over the "native" random coil one, the peptide should contain enough amino acidic residues with the proper acid/basic character and to be oriented in a favorable way to maximize the interaction with the HA surfaces. Nevertheless, it is relevant also to address a number of important weaknesses and assumptions made in the present work due to the limits imposed by the high cost of the adopted B3LYP methodology and of the intrinsic difficulties associated to this problem. First, the charge screening effects due to adsorbed water at the HA surfaces may decrease the favorable interactions of the helix over the random coil conformer and, at the same time, strongly polarize the water molecules directly attached to the surface cations, as shown in a recent work dealing with peptide adsorbed on oxidized silicon and amorphous silica surfaces.[52] In our approach, two H_2O molecules per Ca atom have been considered, which only accounts for a decreased Lewis acidity of each surface cation, the amino acid residues still being able to directly contact the HA Ca^{2+} ions. The question is whether an adsorbed H_2O monolayer might completely exclude the direct contact between surface cations and the amino acid residues. We are not inclined to that possibility as we have shown recently[46] that even glycine (the simplest AA) does prefer to displace water from the HA surface to directly interact with the surface sites rather than being adsorbed on top of a layer of preadsorbed water molecules. Furthermore, recent work using ReaxFF force field by Monti and co-workers[28] shows that during long MD simulations of a fully water solvated glycine and diglycine adsorbed on a TiO_2 surface, water does not displace the amino acids interacting directly with the surface. Second, the entropic contribution to adsorption free energy due to water displacement upon binding has not been considered. As a rough guess, the contact surface area between the peptide and the HA surface is a measure of the amount of displaced water. This quantity is higher for the RC than for the H peptide, which means that the adsorption of the former is entropically favored over the latter one. To what extent this may change the present results is, however, difficult to assess quantitatively. Third, the role of solvent on the folding of free P1 and P2 peptide has not been accounted for here. As expected for such a small peptides, classical MD calculations (Supporting Information Figure S6) revealed a different behavior of the considered peptides in gas phase and in water. That is, a different pool of conformations appeared as a function of the simulation medium, but significantly, all conformations exhibiting a random coil character while helix structures were never present, neither in gas phase nor in solution. As we are interested to see which key interactions are

stabilizing the helix over a random coil (whatever it will be), the main message of this work is therefore preserved. In conclusion, the present results, despite various compromises needed to run large quantum mechanical calculations which prevent from the adoption of fully solvated systems, are in line with the experimental results of Capriotti et al.,[15] where the stabilization of the α-helix conformation induced by HA surfaces of a de novo design peptide rich in γ-carboxyglutamic acid residues was observed.

It is worth mentioning that this work addresses the specific case of HA surfaces as helix-stabilizing substrates; however, other surfaces capable to establish additional interactions that compensate the folding energy costs are also suitable platforms for stabilizing folded conformations. This is, for instance, the case of silica nanoparticles; that is, deprotonated surfaces (with $Si-O^-$ terminations) are able to stabilize helix conformations of arginine- and lysine-rich peptides (in solution, these residues are protonated) due to the strong electrostatic interactions between the partners.[11,12]

■ ASSOCIATED CONTENT

ⓢ Supporting Information

Computational details, supplementary structures, absolute B3LYP energies and coordinates of all considered structures. This material is available free of charge via the Internet at http://pubs.acs.org.

■ AUTHOR INFORMATION

Corresponding Author
*piero.ugliengo@unito.it

Notes
The authors declare no competing financial interest.

■ ACKNOWLEDGMENTS

■ REFERENCES

(1) Cline, D. J.; Thorpe, C.; Schneider, J. P. *J. Am. Chem. Soc.* **2003**, *125*, 2923.

(2) Cox, E. H.; McLendon, G. L. *Curr. Opin. Chem. Biol.* **2000**, *4*, 162.

(3) Kelso, M. J.; Hoang, H. N.; Oliver, W.; Sokolenko, N.; March, D. R.; Appleton, T. G.; Fairlie, D. P. *Angew. Chem., Int. Ed.* **2003**, *42*, 421.

(4) Lombardi, A.; Marasco, D.; Maglio, O.; Di Costanzo, L.; Nastri, F.; Pavone, V. *Proc. Natl. Acad. Sci. U.S.A.* **2000**, *97*, 11922.

(5) Ojida, A.; Inoue, M.-a.; Mito-oka, Y.; Hamachi, I. *J. Am. Chem. Soc.* **2003**, *125*, 10184.

(6) Nicoll, A. J.; Miller, D. J.; Fütterer, K.; Ravelli, R.; Allemann, R. K. *J. Am. Chem. Soc.* **2006**, *128*, 9187.

(7) Le Clainche, L.; Plancque, G.; Amekraz, B.; Moulin, C.; Pradines-Lecomte, C.; Peltier, G.; Vita, C. *J. Biol. Inorg. Chem.* **2003**, *8*, 334.

(8) Jackson, D. Y.; King, D. S.; Chmielewski, J.; Singh, S.; Schultz, P. G. *J. Am. Chem. Soc.* **1991**, *113*, 9391.

(9) Long, J. R.; Oyler, N.; Drobny, G. P.; Stayton, P. S. *J. Am. Chem. Soc.* **2002**, *124*, 6297.

(10) Dolain, C.; Hatakeyama, Y.; Sawada, T.; Tashiro, S.; Fujita, M. *J. Am. Chem. Soc.* **2010**, *132*, 5564.

(11) Lundqvist, M.; Nygren, P.; Jonsson, B.-H.; Broo, K. *Angew. Chem., Int. Ed.* **2006**, *45*, 8169.

(12) Nygren, P.; Lundqvist, M.; Broo, K.; Jonsson, B.-H. *Nano Lett.* **2008**, *8*, 1844.

(13) Fillon, Y.; Verma, A.; Ghosh, P.; Ernenwein, D.; Rotello, V. M.; Chmielewski, J. *J. Am. Chem. Soc.* **2007**, *129*, 6676.

(14) Verma, A.; Nakade, H.; Simard, J. M.; Rotello, V. M. *J. Am. Chem. Soc.* **2004**, *126*, 10806.

(15) Capriotti, L. A.; Beebe, T. P.; Schneider, J. P. *J. Am. Chem. Soc.* **2007**, *129*, 5281.

(16) Baugh, L.; Weidner, T.; Baio, J. E.; Nguyen, P.-C. T.; Gamble, L. J.; Stayton, P. S.; Castner, D. G. *Langmuir* **2010**, *26*, 16434.

(17) Goobes, G.; Goobes, R.; Schueler-Furman, O.; Baker, D.; Stayton, P. S.; Drobny, G. P. *Proc. Natl. Acad. Sci. U.S.A.* **2006**, *103*, 16083.

(18) Goobes, G.; Goobes, R.; Shaw, W. J.; Gibson, J. M.; Long, J. R.; Raghunathan, V.; Schueler-Furman, O.; Popham, J. M.; Baker, D.; Campbell, C. T.; Stayton, P. S.; Drobny, G. P. *Magn. Reson. Chem.* **2007**, *45*, S32.

(19) Masica, D. L.; Gray, J. J.; Shaw, W. J. *J. Phys. Chem. C* **2011**, *115*, 13775.

(20) Peczuh, M. W.; Hamilton, A. D. *Chem. Rev.* **2000**, *100*, 2479.

(21) Wächtershäuser, G. *Proc. Natl. Acad. Sci. U.S.A.* **1990**, *87*, 200.

(22) Cody, G. D.; Boctor, N. Z.; Filley, T. R.; Hazen, R. M.; Scott, J. H.; Sharma, A.; Yoder, H. S. *Science* **2000**, *289*, 1337.

(23) Makrodimitris, K.; Masica, D. L.; Kim, E. T.; Gray, J. J. *J. Am. Chem. Soc.* **2007**, *129*, 13713.

(24) Ghiringhelli, L. M.; Hess, B.; van der Vegt, N. F. A.; Delle Site, L. *J. Am. Chem. Soc.* **2008**, *130*, 13460.

(25) Calzolari, A.; Cicero, G.; Cavazzoni, C.; Di Felice, R.; Catellani, A.; Corni, S. *J. Am. Chem. Soc.* **2010**, *132*, 4790.

(26) Di Felice, R.; Corni, S. *J. Phys. Chem. Lett.* **2011**, *2*, 1510.

(27) van Duin, A. C. T.; Dasgupta, S.; Lorant, F.; Goddard, W. A. *J. Phys. Chem. A* **2001**, *105*, 9396.

(28) Monti, S.; van Duin, A. C. T.; Kim, S.-Y.; Barone, V. *J. Phys. Chem. C* **2012**, *116*, 5141.

(29) Rahaman, O.; van Duin, A. C. T.; Goddard, W. A.; Doren, D. J. *J. Phys. Chem. B* **2010**, *115*, 249.

(30) Bush, I. J.; Tomic, S.; Searle, B. G.; Mallia, G.; Bailey, C. L.; Montanari, B.; Bernasconi, L.; Carr, J. M.; Harrison, N. M. *Proc. R. Soc. A* **2011**, *467* (2131), 2112.

(31) Becke, A. D. *J. Chem. Phys.* **1993**, *98*, 5648.

(32) Dovesi, R.; Saunders, V. R.; Roetti, C.; Orlando, R.; Zicovich-Wilson, C. M.; Pascale, F.; Civalleri, B.; Doll, K.; Harrison, N. M.; Bush, I. J.; D'Arco, P.; Llunell, M. *CRYSTAL09*; University of Torino: Torino, 2009.

(33) Dovesi, R.; Orlando, R.; Civalleri, B.; Roetti, C.; Saunders, V. R.; Zicovich-Wilson, C. M. *Z. Kristallogr.* **2005**, *220*, 571.

(34) Lee, C.; Yang, W.; Parr, R. G. *Phys. Rev. B* **1988**, *37*, 785.

(35) Corno, M.; Rimola, A.; Bolis, V.; Ugliengo, P. *Phys. Chem. Chem. Phys.* **2010**, *12*, 6309.

(36) Schafer, A.; Horn, H.; Ahlrichs, R. *J. Chem. Phys.* **1992**, *97*, 2571.

(37) Rimola, A.; Civalleri, B.; Ugliengo, P. *Phys. Chem. Chem. Phys.* **2010**, *12*, 6357.

(38) Grimme, S. *J. Comput. Chem.* **2006**, *27*, 1787.

(39) Civalleri, B.; Zicovich-Wilson, C. M.; Valenzano, L.; Ugliengo, P. *CrystEngComm* **2008**, *10*, 405.

(40) Oostenbrink, C.; Villa, A.; Mark, A. E.; van Gunsteren, W. F. *J. Comput. Chem.* **2004**, *25*, 1656.

(41) van Der Spoel, D.; Lindahl, E.; Hess, B.; Groenhof, G.; Mark, A. E.; Berendsen, H. J. *J. Comput. Chem.* **2005**, *26*, 1701.

(42) Berendsen, H. J. C.; Postma, J. P. M.; van Gunsteren, W. F.; DiNola, A.; Haak, J. R. *J. Chem. Phys.* **1984**, *81*, 3684.

(43) Hess, B.; Bekker, H.; Berendsen, H. J. C.; Fraaije, J. G. E. M. *J. Comput. Chem.* **1997**, *18*, 1463.

(44) Amadei, A.; Linssen, A. B.; Berendsen, H. J. C. *Proteins* **1993**, *17*, 412.

(45) Rimola, A.; Corno, M.; Zicovich-Wilson, C. M.; Ugliengo, P. *J. Am. Chem. Soc.* **2008**, *130*, 16181.

(46) Rimola, A.; Corno, M.; Zicovich-Wilson, C. M.; Ugliengo, P. *Phys. Chem. Chem. Phys.* **2009**, *11*, 9005.

(47) Rimola, A.; Sakhno, Y.; Bertinetti, L.; Lelli, M.; Martra, G.; Ugliengo, P. *J. Phys. Chem. Lett.* **2011**, *2*, 1390.

(48) Rimola, A.; Corno, M.; Garza, J.; Ugliengo, P. *Philos. Trans. R. Soc., A* **2012**, *370*, 1478.

(49) Ramaekers, R.; Pajak, J.; Lambie, B.; Maes, G. *J. Chem. Phys.* **2004**, *120*, 4182.

(50) Corno, M.; Orlando, R.; Civalleri, B.; Ugliengo, P. *Eur. J. Mineral.* **2007**, *19*, 757.

(51) Corno, M.; Busco, C.; Bolis, V.; Tosoni, S.; Ugliengo, P. *Langmuir* **2009**, *25*, 2188.

(52) Schneider, J.; Ciacchi, L. C. *J. Am. Chem. Soc.* **2012**, *134*, 2407.